

**Magnetic structure and orbital ordering in BaCoO<sub>3</sub> from first-principles calculations**V. Pardo,<sup>1,2,3,\*</sup> P. Blaha,<sup>2</sup> M. Iglesias,<sup>1,3</sup> K. Schwarz,<sup>2</sup> D. Baldomir,<sup>1,3</sup> and J. E. Arias<sup>3</sup><sup>1</sup>*Departamento de Física Aplicada, Facultad de Física, Universidad de Santiago de Compostela, E-15782 Campus Sur s/n, Santiago de Compostela, Spain*<sup>2</sup>*Institute for Materials Chemistry, Vienna University of Technology, Getreidemarkt 9/165, A-1060 Vienna, Austria*<sup>3</sup>*Instituto de Investigaciones Tecnológicas, Universidad de Santiago de Compostela, E-15782, Santiago de Compostela, Spain*

(Received 15 April 2004; published 29 October 2004)

*Ab initio* calculations using the APW+lo method as implemented in the WIEN2k code have been used to describe the electronic structure of the quasi-one-dimensional system BaCoO<sub>3</sub>. Both, GGA and LDA+*U* approximations were employed to study different orbital and magnetic orderings. GGA predicts a metallic ground state whereas LDA+*U* calculations yield an insulating and ferromagnetic ground state (in a low-spin state) with an alternating orbital ordering along the Co-Co chains, consistent with the available experimental data.

DOI: 10.1103/PhysRevB.70.144422

PACS number(s): 75.25.+z, 71.15.Ap, 71.15.Mb, 71.20.-b

**I. INTRODUCTION**

In the past few years, the main interest in Co oxides has been their applications in solid state fuel cells.<sup>1</sup> Furthermore, some mixed valence Co compounds showed interesting colossal magnetoresistance (CMR) effects.<sup>2</sup> Very recently, a renewed interest in Co oxides started after the discovery of the first Co-based superconductor.<sup>3</sup> Due to these two phenomena, CMR and superconductivity, Co oxides are of great interest from a physical point of view. Most of the interesting physical properties in transition metal oxides lie in the interplay between electronic structure and magnetic properties. New experimental techniques allow to investigate the coupling between magnetic and orbital degrees of freedom, which plays a major role in this type of materials.<sup>4-6</sup>

BaCoO<sub>3</sub> is a transition metal oxide with interesting properties, which have been studied in recent years.<sup>7-10</sup> In its highly anisotropic structure, face-sharing CoO<sub>6</sub> octahedra form chains that are likely to produce one-dimensional effects in its magnetic properties. The hexagonal structure, however, may lead to magnetic frustration when the Co atoms perpendicular to the chains (on a triangular arrangement) should have an antiferromagnetic coupling.

The experimental studies on BaCoO<sub>3</sub> have established that the Co ions are in a low-spin state ( $S=1/2$ ),<sup>7</sup> as to be expected for a Co<sup>4+</sup> ion, with the configuration  $t_{2g}^5 e_g^0$  in the case of octahedral symmetry. In the temperature range from 70 to 300 K, the material is found to be semiconducting, with conduction occurring through *n*-type carriers.<sup>7</sup> The origin of the gap is not yet resolved.<sup>8</sup> Possible reasons are a Mott-Hubbard-type transition, an Anderson localization due to some structural disorder or a “Peierls” dimerization of the Co chains, but none have been confirmed experimentally.

First measurements reported a Néel temperature  $T_N=8$  K,<sup>11</sup> but recent experiments reveal a more complex magnetic structure<sup>7</sup> beyond the simple antiferromagnetic behavior. Paramagnetism is found above 250 K, where a coupling constant of  $J/k_B=10$  K is estimated by fitting to a one-dimensional (1D) Heisenberg model. For temperatures between 70 and 250 K, ferromagnetic coupling is predomi-

nant, whereas for  $T<70$  K antiferromagnetic couplings become more important. Unfortunately no neutron diffraction data are available and the magnetic order at very low temperatures is not known. Also the relative strengths of intrachain and interchain magnetic couplings are still uncertain.

In this paper, we try to shed some light into the electronic structure of BaCoO<sub>3</sub> by means of *ab initio* full-potential augmented plane wave plus local orbitals (APW+lo) calculations<sup>12</sup> carried out with the WIEN2k code.<sup>13,14</sup> We study some possible magnetic and orbital orderings (Sec. II) and investigate the electronic structure from our *ab initio* calculations (Sec. III). In Sec. IV we present the results from the standard GGA calculations and in Sec. V we try to incorporate electron correlation effects by means of the LDA+*U* approximation.

**II. STRUCTURE AND MAGNETIC ORDERINGS**

BaCoO<sub>3</sub> crystallizes in the hexagonal-2H pseudo-perovskite structure with space group  $P6_3/mmc$ , and lattice parameters  $a=5.645$  Å and  $c=4.752$  Å.<sup>15</sup> The position of the oxygen atoms has a free structural parameter whose value was taken from Ref. 9 where it has been obtained from LAPW calculations.

Figure 1 shows that BaCoO<sub>3</sub> forms chains of face-sharing CoO<sub>6</sub> octahedra with a much shorter ( $\approx 2.38$  Å) Co-Co distance along the *c* axis than between the chains ( $\approx 5.65$  Å), giving the structure a strong 1D character. The Co chains are organized in a triangular manner, giving rise to magnetic frustration when one assumes antiferromagnetism within the plane perpendicular to the Co chains and restricts to collinear magnetism. The Ba ion acts merely as an electron donor.

In Fig. 2 we show the different magnetic orderings studied in this work. Besides a ferromagnetic (FM) ordering [Fig. 2(a)] also an “A-type” antiferromagnetic (AF) order is possible, where FM hexagonal planes are coupled antiferromagnetically [Fig. 2(b)]. The triangular geometry of the Co chains leads to magnetic frustration of any possible collinear AF long-range order in the hexagonal plane (perpendicular to the chains).<sup>16</sup> Nevertheless, we have studied two partly AF

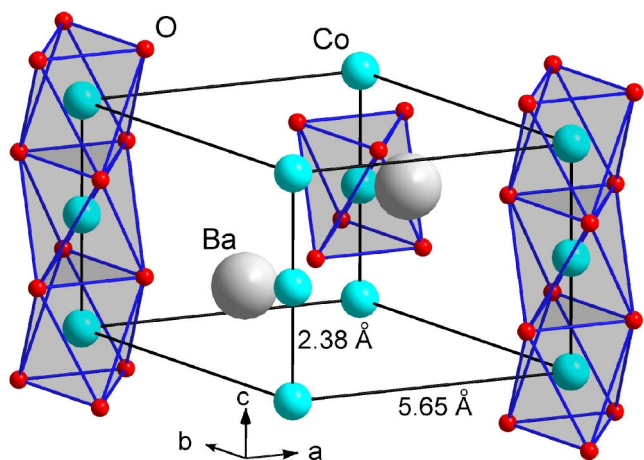


FIG. 1. (Color online) Hexagonal structure of  $\text{BaCoO}_3$ . Observe the chains of face-sharing  $\text{CoO}_6$  octahedra and the triangular arrangement of these chains forming a hexagonal structure.

arrangements, where each Co has 2 FM and 4 AF neighbors within the hexagonal plane. These planes can be coupled antiferromagnetically [AF-type I, Fig. 2(c)] or ferromagnetically [AF-type II, Fig. 2(d)] along the  $c$  axis.

We study these different configurations mainly in order to explore the relative strength of interchain with respect to the intrachain magnetic interactions. The quasi-one-dimensional structure of the compound would imply that the intrachain magnetic coupling is most important, since the corresponding Co-Co distance is more than two times smaller than the interchain Co-Co distance.

### III. COMPUTATIONAL DETAILS

All calculations in this paper were carried out with the WIEN2k package.<sup>13,14</sup> This uses the full-potential APW+lo method<sup>12</sup> that makes no shape approximation to the potential or density. Local orbitals (Co  $3s$ ,  $3p$ ,  $3d$ , Ba  $4d$ ,  $5s$ ,  $5p$ , O  $2s$

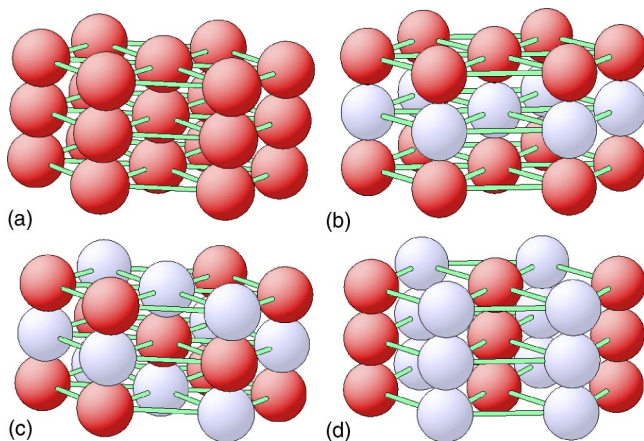


FIG. 2. (Color online) Different magnetic configurations of  $\text{BaCoO}_3$  studied. Only Co atoms are shown, dark (light) spheres indicate spin up (down) character. (a) FM; (b) A-type AF (FM in plane, AF between planes); (c) AF-type I (AF along  $c$ ); (d) AF-type II (FM along  $c$ ).

and  $2p$ ) were added to improve the flexibility of the basis set and to describe semicore states. The values of the atomic sphere radii ( $R_{mt}$ ) were chosen as 1.70 a.u. for Co, 2.0 a.u. for Ba, and 1.55 a.u. for O.

We calculated the properties of the system within both the generalized gradient approximation (GGA) using the PBE scheme<sup>17</sup> and the LDA+ $U$  approximation.<sup>18–20</sup> In the latter, the DFT (orbital independent) part of the potential was treated by the same GGA scheme. For GGA, we explored the energy vs magnetic moment in the range  $S=0$  to  $S=1/2$  using the fixed spin moment (FSM) method<sup>21</sup> that fixes the total magnetic moment in the unit cell. We used a plane wave cutoff described by  $R_{mt}K_{\max}=7$  and 72  $k$  points in the irreducible Brillouin zone (IBZ) (1000  $k$  points in the whole Brillouin zone). Convergence was checked up to  $R_{mt}K_{\max}=8$  and 150  $k$  points in the IBZ. For the larger AF unit cells, equivalent  $k$  meshes were employed.

The use of the LDA+ $U$  method is especially suited for this moderately correlated transition metal oxide, since it allows to introduce an on-site Coulomb repulsion term, characterized by a Hubbard  $U$ . In addition, the introduction of an orbital dependent potential allows to study orbital orderings, which turn out to be an important issue in this class of compounds.

## IV. GGA CALCULATIONS

### A. FSM curve

In order to investigate the magnetic properties of the present compound, we analyzed the energy of the FM system by varying the magnetic moment of the cell. In a previous paper<sup>10</sup> it was shown that the low-spin (LS) state has a much lower energy than possible high-spin states. In the present paper, however, we explore the magnetic solutions around the experimentally found LS state and investigate them in more detail. The unit cell contains two Co ions, and thus the expected total magnetic moment for a perfect LS state of Co would be  $2\mu_B$ . For this purpose we used the FSM method within the GGA approximation for the exchange-correlation potential. This method allows to calculate the total energy as a function of the fixed total magnetization in the unit cell.<sup>21</sup>

The results are shown in Fig. 3, where the minimum of the FSM curve is located near (at around  $1.5\mu_B$  per unit cell) but definitely below the LS state. Only about  $0.5\mu_B$  comes from inside each Co sphere, but the rest of the magnetic moment resides inside the O spheres and the interstitial region. The LS state would imply a half-metallic electronic structure, i.e., a gap in the spin-up, but a metallic spin-down DOS, in contrast to the experimentally observed semiconducting behavior, which cannot be obtained within GGA for the FM case.

Figure 4 shows how the DOS curves change when the total magnetic moment is varied from 0 to  $2\mu_B$ . Half-metallicity is reached when the magnetic moment per Co site is set to an integer value. The spin-down compared to the spin-up DOS is approximately shifted rigidly.

These results roughly agree with LMTO-ASA calculations,<sup>8</sup> which find the ground state to be a FM low-spin state. They find, however, a much higher stabilization

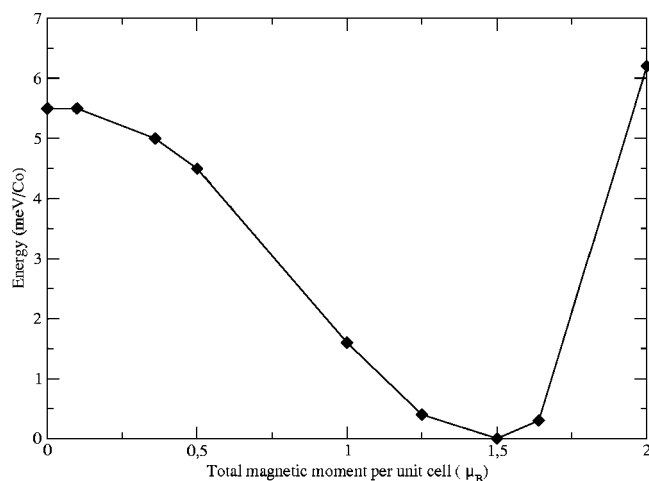


FIG. 3. Energy vs magnetic moment by FSM calculation using GGA. The minimum is near  $1.5\mu_B$  while the perfect LS state ( $2\mu_B$ ) is comparable in energy to the nonmagnetic state. The line is a guide for the eye.

for that state with respect to the nonmagnetic case, which is probably due to the atomic sphere approximation (ASA).

### B. Antiferromagnetic calculations

The nonsymmorphic symmetry operations involving a translation of  $(0,0,1/2)$  along the Co chains cause degener-

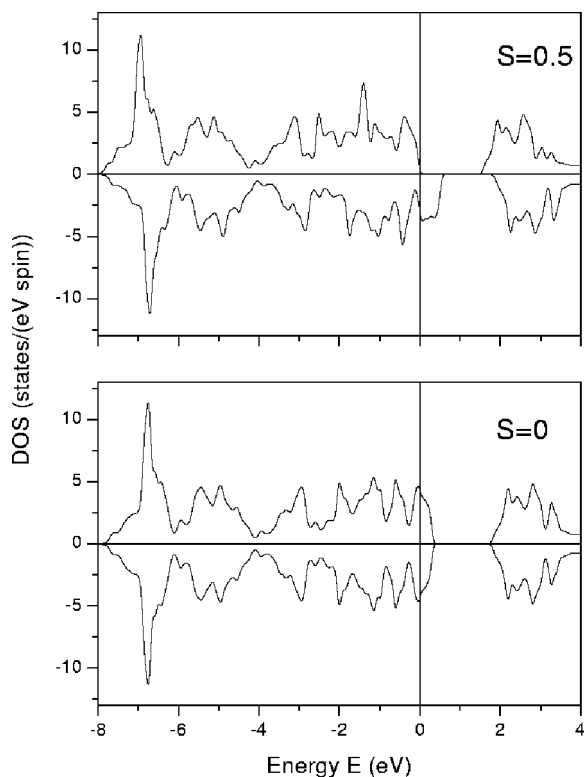


FIG. 4. Total spin-up and spin-down DOS (shown at the positive and negative scale) within GGA for fixed values of the total magnetic moment per unit cell of 0 and  $2\mu_B$ , with  $S=0$  and  $S=0.5$ , respectively.

TABLE I. Relative energies (with respect to the FM ground state) of the different magnetic configurations studied with GGA. The value of the magnetic moment is for the Co atom within its atomic sphere.

	Energy (meV/Co)	Magnetic moment ( $\mu_B$ )
Ferromagnetic	0	0.48
Nonmagnetic	5.5	0.0
AF-type II	5.8	0.11

ate bands that appear near the Fermi level. To get an insulating behavior those degenerate bands must be split by breaking this symmetry, e.g., with an antiferromagnetic order. Within GGA calculations, the A-type AF order is unstable and converges to a nonmagnetic solution. Among the cases studied here, the only AF structure that converges to a solution different from a nonmagnetic case is the AF-type II structure [see Fig. 2(d)]. This ordering assumes a partial AF coupling of FM Co chains. The in-plane coupling is FM along the  $b$  axis, leading to two FM but four AF nearest neighbors. This solution has a fairly small magnetic moment on the Co sites, of just  $0.11\mu_B$  per Co sphere. Although the Co chains are quite far apart, we obtain a much smaller moment with this partly AF coupling than the completely FM aligned case ( $0.48\mu_B$  per Co sphere). Apparently the inter-chain coupling is stronger than one would intuitively assume according to the quasi-one-dimensional structure of the material. The energy of the AF-type II structure is higher than the FM case, which is the most stable solution within GGA, and is even higher than a nonmagnetic solution (see Table I). We see that the energy differences involved are fairly small.

### C. Peierls distortion

The question remains, namely which mechanism can open a gap around the Fermi level and yield the experimentally observed semiconducting state. A possible mechanism investigated in Ref. 8 would be a dimerization of the Co atoms along the chains via a Peierls distortion. In order to simulate it, we displace one of the Co atoms in the Co chains along the  $c$  axis towards the other Co to form dimers, i.e., one Co is displaced from the equilibrium position halfway between the other type of Co atoms, which are at the corners of the unit cell (see Fig. 1). For this constrained Co displacement, the positions of the oxygen and barium atoms were relaxed by minimizing the forces acting on them.

Even at very high distortions, we did not observe a semiconducting state, contrary to the results from LMTO-ASA calculations<sup>8</sup> (probably because these authors did not fully relax the O and Ba atoms). We take oxygen relaxation into account and observe a flattening of the bands around the Fermi level, but the hybridization makes the bands broad enough to overlap causing a metallic behavior. We observe a decrease in the total magnetic moment per unit cell from  $1.5\mu_B$  in the symmetric case to  $1.3\mu_B$  in the most distorted case studied. Since the corresponding energies are high, we can conclude that in this system a Peierls distortion is not likely to occur. A small Co distortion of  $0.07 \text{ \AA}$  from the

TABLE II. Main results for the different magnetic configurations studied within LDA+ $U$  ( $U=5$  eV). Orbital order labelled “alt.  $c$ ” means that the hole is alternating between  $d_{x^2-y^2}$  and  $d_{xy}$  orbitals in Co atoms along the Co chain, “alt.  $ab$ ” means that it is alternating within the hexagonal  $ab$  plane. The magnetic moments  $M$  correspond to the amount of the moment that resides inside the atomic spheres specified.

Magnetic order	Orbital order	Energy (meV/Co)	$M(\text{Co1})$ ( $\mu_B$ )	$M(\text{Co2})$ ( $\mu_B$ )	Insulator
FM	alt. $c$	0	0.846	0.850	Yes
	$d_{x^2-y^2}$	71	0.698	0.698	No
	$d_{xy}$	76	0.705	0.705	No
A-type AF	alt. $c$	7	0.688	-0.689	Yes
	$d_{x^2-y^2}$	52	0.768	-0.767	Yes
	$d_{xy}$	54	0.770	-0.770	Yes
Nonmagnetic	None	58	0	0	No
AF-type I	alt. $c$	12	0.811	-0.818	Yes
	$d_{x^2-y^2}$	58	0.897	-0.897	Yes
	$d_{xy}$	57	0.900	-0.900	Yes
AF-type II	alt. $ab$	86	0.651	-0.674	No
	$d_{x^2-y^2}$	93	0.683	-0.683	No
	$d_{xy}$	93	0.682	-0.682	No

equilibrium raises the energy by 71 meV/Co but a larger distortion (of 0.32 Å) by 1 eV/Co. In the earlier band structure study,<sup>9</sup> it has been shown that no Fermi surface nesting is present.

## V. LDA+ $U$ CALCULATIONS

In the preceding sections we have shown that it is not possible to find an insulating behavior within GGA, not even by symmetry breaking. The LDA+ $U$  method within the so-called “fully localized limit”<sup>20</sup> is an approximation that allows to treat the strong electron-electron interactions that occur in transition metal oxides. This method is known to improve over GGA in these highly correlated transition metal oxides and to predict better values of the magnetic moments and gaps. A good overview of this method is given in Ref. 19.

The method needs two input parameters, the on-site Coulomb repulsion  $U$  and the exchange energy  $J$ . The value of  $J$  was taken as the average energy shift between spin-up and spin-down bands of the GGA spin-polarized calculation (approximately 0.5 eV). As shown recently<sup>22</sup> the exact value of  $U$  depends on the computational method and the approximations made when estimating  $U$ . However, it is generally agreed that for this type of compound the value of  $U$  is in the range of several eV up to about 8 eV. In the present study we assumed  $U$  to be 5 eV, but checked how the results depend on  $U$  and found that for  $U=2.5$  eV, we basically recover the GGA solution. For larger values of  $U$  (6 eV and 7 eV), the

FM solution remains stable with a total magnetic moment of  $1.00\mu_B$  per Co ion, but the energy difference between the FM and AF solutions gets gradually reduced as  $U$  increases. Also, the magnetic moments get more localized inside the atomic spheres as  $U$  increases, as expected. We want to stress that all our conclusions in this paper do not depend on  $U$  as long as it is chosen in a reasonable range.

### A. Possible magnetic and orbital orderings

We investigated the different magnetic configurations shown in Fig. 2 using the LDA+ $U$  method. In this case, a magnetic solution is possible for all structures, with strongly localized spin moments on the Co sites and negligible contributions from the other spheres. The main results are summarized in Table II.

$\text{Co}^{4+}$  in a (nearly) octahedral environment would be a  $t_{2g}^5 e_g^0$  system with one hole in the spin-down  $t_{2g}$  states. In the present hexagonal crystal structure, these are the  $d_{z^2}$ ,  $d_{xy}$ , and  $d_{x^2-y^2}$  orbitals, whereas the  $d_{xz}$  and  $d_{yz}$  orbitals form the  $e_g$  manifold pointing towards the O ligands. It turns out that within LDA+ $U$  the hole can be localized predominantly in the  $d_{x^2-y^2}$  and/or  $d_{xy}$  orbitals, but never in the  $d_{z^2}$  state, which is always fully occupied. From Table II, we see that the energy difference between solutions with a  $d_{x^2-y^2}$  or  $d_{xy}$  hole is very small, but both are much higher than the solution with an alternating orbital ordering (i.e., Co atoms along the Co chain have alternating  $d_{x^2-y^2}$  and  $d_{xy}$  holes). This energy gain is much larger than the differences between different mag-

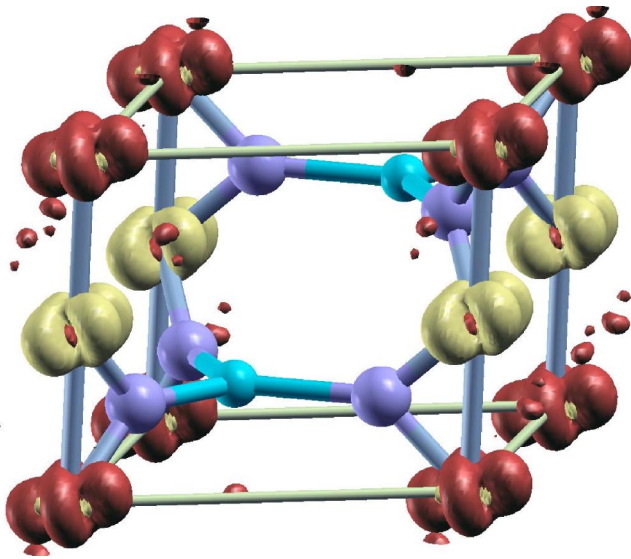


FIG. 5. (Color online) Spin density plot [isosurface at  $0.2 e/\text{\AA}^3$  produced using XCrySDen (Ref. 23)] for the alternating orbital ordered A-type AF configuration. The spin moment is located in  $d_{x^2-y^2}$  and  $d_{xy}$  orbitals alternating along the Co chains (the orbitals form angles of 45 degrees with each other). The FM orbital-ordered solution would be similar but all Co atoms would have same spin (equal color).

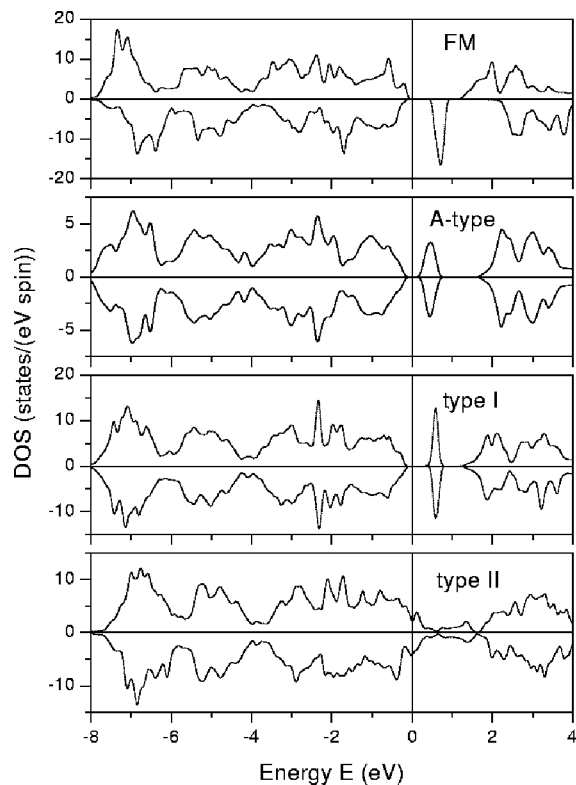


FIG. 6. Total spin-up/down density of states (DOS) within LDA+ $U$  for the different magnetic configurations in the alternating orbital ordered state. Semiconducting behavior is related to symmetry breaking along the Co chains. The energy is taken with respect to  $E_F$ .

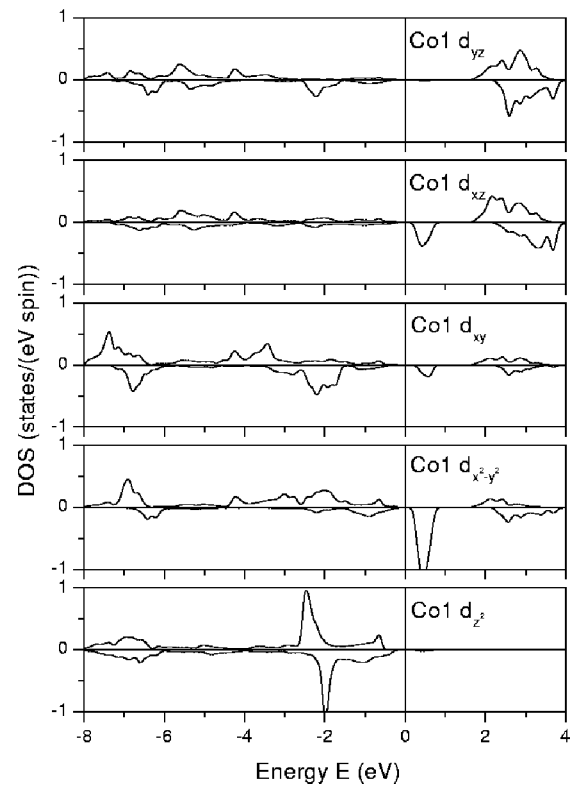


FIG. 7. Partial spin-up/down Co  $d$  DOS for the Co1 atom in a ferromagnetic, alternating orbital ordered case (within LDA+ $U$ ). The hole is located at the  $d_{x^2-y^2}$  orbital.

netic orderings (FM vs A-type AF or AF-type I or even a nonmagnetic solution). Therefore, magnetic configurations play a minor role in this quasi-one-dimensional system. This finding is consistent with the results in Ref. 24 where it was shown that this type of orbital ordering is caused by superexchange interactions in a frustrated Jahn-Teller system with metal-oxygen-metal bonds of  $90^\circ$ . In  $\text{BaCoO}_3$ , this angle is  $86.9^\circ$  and thus spin and orbital degrees of freedom are decoupled, making the spin exchange much weaker than the orbital one.

The A-type AF structure is the most stable antiferromagnetic configuration studied here. It is the only one that can lead to a collinear long-range AF ordering (along the Co chains). As mentioned above, the energy difference to the FM ground state decreases with increasing  $U$ .

In the AF-type II case we restricted the Co atoms to be equivalent within the chain, and allowed orbital order only between the chains. Even this case of interchain orbital ordering is energetically favorable (though not as much as within the Co chain). Once again this is a sign for sizable interchain interactions, which are not expected to be that large in a quasi-one-dimensional system.

For the FM case, an alternating orbital ordering along the chains removes the symmetry that makes the two types of Co atoms along  $c$  equivalent. This produces an energy gap around the Fermi level, leading to an insulating behavior. Such an insulating state can also be reached when this symmetry is broken by an AF ordering along the chain. In the case of AF-type II, the intrachain symmetry is not broken

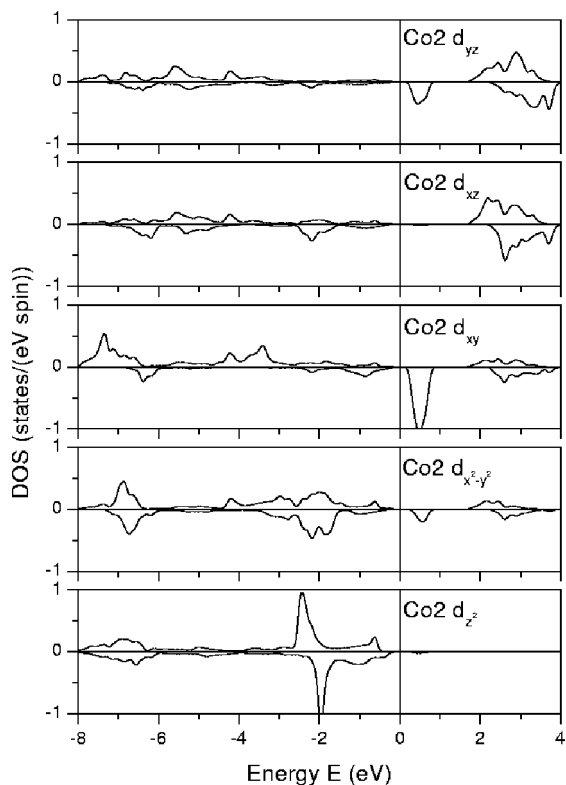


FIG. 8. Partial spin-up/down Co *d* DOS for the Co2 atom in a ferromagnetic, alternating orbital ordered case (within LDA+*U*). The hole is located at the  $d_{xy}$  orbital.

and thus a metallic state remains. Just as in GGA, the FM solution is the most stable in LDA+*U* calculations. In the latter case, the total magnetic moment within the unit cell (which now contains four Co atoms) is  $4.00\mu_B$  for the alternating orbital ordering (which corresponds to the LS state), while it is only  $3.9\mu_B$  for the other orbital orderings (with metallic character).

Figure 5 shows the spin density of the alternating orbital ordered state of the A-type AF structure. The FM case would look similar, but the colors (indicating spin-up and spin-down) would be equal for every Co atom. The spin-density along the Co chains is localized in two orbitals, which are rotated 45 degrees to each other, having their lobes in the hexagonal plane ( $d_{x^2-y^2}$  and  $d_{xy}$ , respectively). In addition we see some spin density on the O atoms indicating the importance of the  $90^\circ$  superexchange mentioned above.

### B. Densities of states (DOS)

In this section we discuss the main features of the electronic structure of the system using the DOS plots. In GGA one obtains (almost) a half-metallic ferromagnet (see upper panel of Fig. 4), where the (distorted) octahedral crystal field dominates and splits the Co *d* states into (mostly) occupied  $t_{2g}$  and empty  $e_g$  manifolds. The additional crystal field due to the distortion of the octahedra is almost negligible compared to the bandwidth and cannot separate the three  $t_{2g}$  orbitals, thus we cannot obtain the experimentally found semi-conducting state, not even when we break the symmetry by a

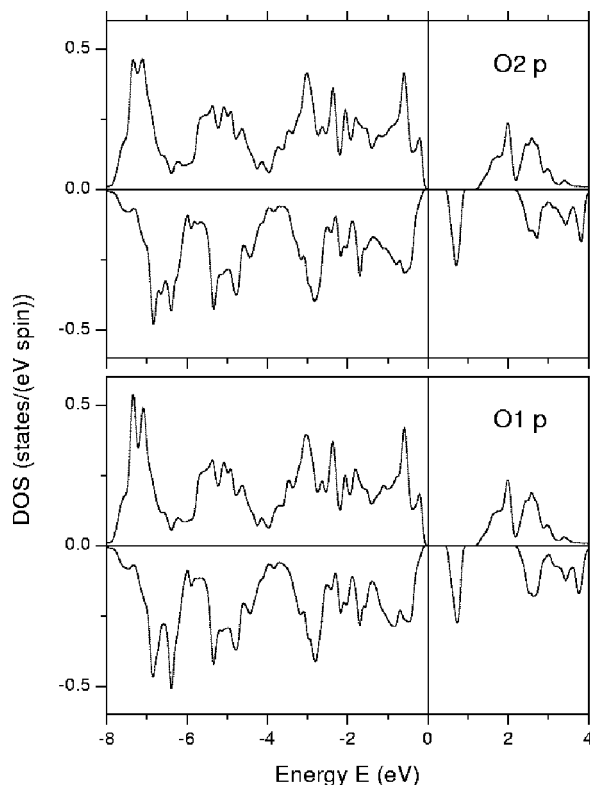


FIG. 9. Partial spin-up/down O *p* DOS for the ferromagnetic, orbital ordered case (within LDA+*U*). Observe that the hole has some O *p* character, which comes from  $p_x$  and  $p_y$  orbitals but has no component along the Co chain axis.

Peierls distortion. The resulting total moment of  $2\mu_B$  per unit cell is fairly delocalized over the entire unit cell and thus leads to a relatively small moment inside the Co spheres (see Table I).

Within the LDA+*U* method, we obtain a physically more plausible solution: the strong local Coulomb correlation lifts the quasidegeneracy of the three  $t_{2g}$  orbitals and the “hole” (see above) is localized in one of them. This leads to an insulating ground state in agreement with experiment and since the Co *d* wave function is now strongly localized, also the corresponding magnetic moments are more localized inside the Co spheres, as expected for a correlated system (see Table II).

In Fig. 6 we show the total DOS for the four magnetic configurations studied within LDA+*U*. All of them are in an alternating orbital ordered configuration, since this is their lowest energy state. The main observation is that insulating behavior is found for the FM, the A-type AF, and AF-type I structures, where alternating orbital ordering occurs along the Co chains. In the AF-type II case we forced the translational symmetry along the Co chains and thus excluded intrachain orbital ordering (we have FM chains coupled AF to some of their neighbors). In this case, no splitting appears in the bands around the Fermi level. Hence, the lowest energy states with an alternating orbital ordering reproduce the experimental evidences, while without this symmetry breaking a metallic solution would occur.

In the case of FM coupling and alternating orbital ordering, we show in Figs. 7 and 8 the partial DOS corresponding

to the different Co  $d$  orbitals for the two types of adjacent Co atoms along the Co chains. For Co1, the hole is mainly located in the  $d_{x^2-y^2}$  orbital with some  $d_{xy}$  and  $d_{xz}$  component (see peaks just above  $E_F$ ), where the latter produces the tilting visible in the spin density shown in Fig. 5. In the case of Co2, the hole is mainly of  $d_{xy}$  character with some admixture (Fig. 8) of  $d_{xy}$  and  $d_{x^2-y^2}$ . The  $e_g$ -like orbitals ( $d_{xz}$  and  $d_{yz}$ ) are predominantly unoccupied while the  $d_{z^2}$  orbital is fully occupied in any case.

In Fig. 9 we observe that the hole found in the total DOS plot has some O  $p$  character as well. This is again a manifestation of the importance of the  $90^\circ$  superexchange mechanism. It is mainly due to the  $p_x$  and  $p_y$  but not due to the  $p_z$  orbital which points along the chain axis. One can see this from Fig. 5 as well, noticing that the O spin cloud is mainly in the plane perpendicular but not along the Co chains.

## VI. SUMMARY

In this paper we carried out *ab initio* density functional theory calculations using the full-potential APW+lo method as implemented in the WIEN2k code on the transition metal oxide BaCoO<sub>3</sub>.

The calculations using GGA for the exchange-correlation potential gave a ferromagnetic configuration as the most stable one. The value of the spin magnetic moment was calculated using the FSM method and the result was  $1.5\mu_B$ /unit cell, smaller than the expected  $2\mu_B$ /unit cell for a perfect LS state. Antiferromagnetic configurations within the Co chain could not be obtained. All GGA solutions are metallic in contrast to the experimental semiconducting state. We inves-

tigated the possibility of a Peierls distortion as a cause for the semiconducting behavior, but had to rule it out by total energy calculations. Thus, crystal field effects alone cannot split the quasidegenerate  $t_{2g}$  orbitals and a metallic state results contrary to experiment.

Within the LDA+ $U$  method, however, we can incorporate the correlation effects due to the Coulomb interactions among the Co  $3d$  electrons and this results in a splitting of the degenerate  $t_{2g}$  states and yields an insulator. We studied different magnetic and orbital orderings and found that an intrachain alternating orbital ordering with FM coupling is the most stable solution. The orbital ordering is caused by a nearly  $90^\circ$  superexchange mechanism of the face-sharing octahedra and leads to the main stabilization, whereas the magnetic order is of secondary importance. In addition, this orbital ordering produces an insulating solution, which reproduces the experimental observations.

Our electronic structure calculations indicate that the interchain couplings are weak but stronger than expected for a nearly 1D system.

## ACKNOWLEDGMENTS

V.P., M.I., D.B., and J.E.A. wish to thank the CESGA (Centro de Supercomputación de Galicia) for the computing facilities, J. Rivas and J. Castro for fruitful discussions and also acknowledge the Xunta de Galicia for the financial support through the project PGIDIT02TMT20601PR. V. P. wishes to thank the Xunta de Galicia for the financial support. P.B. acknowledges the support by the Austrian Science Fund (FWF), Project No. P14699-TPH.

\*Electronic address: vpardo@usc.es

<sup>1</sup>T. Ishihara, S. Fukui, H. Nishiguchi, and Y. Takita, *J. Electrochem. Soc.* **149**, A823 (2002).  
<sup>2</sup>C. Martin, A. Maignan, D. Pelloquin, N. Nguyen, and B. Raveau, *Appl. Phys. Lett.* **71**, 1421 (1997).  
<sup>3</sup>K. Takada, H. Sakurai, E. Takayama-Muromachi, F. Izumi, R. Dilanian, and T. Sasaki, *Nature (London)* **422**, 53 (2003).  
<sup>4</sup>G. Maris, Y. Ren, V. Volotchaev, C. Zobel, T. Lorenz, and T. Palstra, *Phys. Rev. B* **67**, 224423 (2003).  
<sup>5</sup>M. Takata, E. Nishibori, K. Kato, M. Sakata, and Y. Moritomo, *J. Phys. Soc. Jpn.* **68**, 2190 (1999).  
<sup>6</sup>S. Dhesi *et al.*, *Phys. Rev. Lett.* **92**, 056403 (2004).  
<sup>7</sup>K. Yamaura, H. Zandbergen, K. Abe, and R. Cava, *J. Solid State Chem.* **146**, 96 (1999).  
<sup>8</sup>C. Felser, K. Yamaura, and R. Cava, *J. Solid State Chem.* **146**, 411 (1999).  
<sup>9</sup>V. Pardo, M. Iglesias, D. Baldomir, J. Castro, and J. Arias, *Solid State Commun.* **128**, 101 (2003).  
<sup>10</sup>J. L. Cacheiro, M. Iglesias, V. Pardo, D. Baldomir, and J. Arias, *Int. J. Quantum Chem.* **91**, 252 (2003).  
<sup>11</sup>Y. Takeda, *J. Solid State Chem.* **15**, 40 (1975).  
<sup>12</sup>E. Sjöstedt, L. Nördstrom, and D. Singh, *Solid State Commun.* **114**, 15 (2000).  
<sup>13</sup>K. Schwarz and P. Blaha, *Comput. Mater. Sci.* **28**, 259 (2003).

<sup>14</sup>P. Blaha, K. Schwarz, G. K. H. Madsen, D. Kvasnicka, and J. Luitz, *WIEN2k, An Augmented Plane Wave Plus Local Orbitals Program for Calculating Crystal Properties* (Vienna University of Technology, Austria, 2001).  
<sup>15</sup>H. Taguchi, Y. Takeda, F. Kanamaru, M. Shimada, and M. Koizumi, *Acta Crystallogr., Sect. B: Struct. Crystallogr. Cryst. Chem.* **B33**, 1299 (1977).  
<sup>16</sup>M. Mao, B. Gaulin, R. Rogge, and Z. Tun, *Phys. Rev. B* **66**, 184432 (2002).  
<sup>17</sup>J. Perdew, S. Burke, and M. Ernzerhof, *Phys. Rev. Lett.* **77**, 3865 (1996).  
<sup>18</sup>A. Lichtenstein, V. Anisimov, and J. Zaanen, *Phys. Rev. B* **52**, R5467 (1995).  
<sup>19</sup>V. Anisimov, F. Aryasetiawan, and A. Lichtenstein, *J. Phys.: Condens. Matter* **9**, 767 (1997).  
<sup>20</sup>A. Petukhov, I. Mazin, L. Chioncel, and A. Lichtenstein, *Phys. Rev. B* **67**, 153106 (2003).  
<sup>21</sup>K. Schwarz and P. Mohn, *J. Phys. F: Met. Phys.* **14**, L129 (1984).  
<sup>22</sup>M. Cococcioni and S. de Gironcoli, cond-mat/0405160 (unpublished).  
<sup>23</sup>A. Kokalj, *J. Mol. Graphics Modell.* **17**, 176 (1999).  
<sup>24</sup>M. Mostovoy and D. Khomskii, *Phys. Rev. Lett.* **89**, 227203 (2002).